A discrete element approach for modelling bendable crop stems

Tom Leblicq[a,*], Bart Smeets[a], Simon Vanmaercke[a], Herman Ramon[a], Wouter Saeys[a]

[a]*KU Leuven - University of Leuven, Department of Biosystems (BIOSYST), Division of Mechatronics, Biostatistics and Sensors (MeBioS), Kasteelpark Arenberg 30, 3001 Leuven, Belgium*

Abstract

A requirement for optimizing crop processing machinery using DEM simulations is the application of virtual stems that behave realistically during deformation. In this study, data based bending models were developed for virtual segmented crop stems. These models combine realistic bending behaviour with a minimal number of model parameters. Also the effects of plastic deformation and damage were incorporated in the model. The bending model was successfully used to validate the bending behaviour of individual stems through comparison of simulations and validation measurements. It was also shown that the model is suitable for virtual stems with different numbers of segments. Moreover, based on a stem measurement it could be predicted what would happen to the same stem if it would have other dimensions or if it would be supported at different locations. Additional stem measurements were used to validate this. No significant difference ($\alpha = 0.05$) was observed between measurements and simulations. Finally, pendulum exper-

*Corresponding author.
Tel.: +32 16 377 116; E-mail address: tom.leblicq@biw.kuleuven.be

iments showed that the deformation rate has no significant effect ($\alpha = 0.05$) on the deformation behaviour of individual crop stems.
Keywords: DEM, Simulation, Bending model, Lookup table, Wheat

1. Introduction

Stem crops are harvested by rotary mowers and by combine and forage harvesters. Collecting the crop residues is done with loader wagons and balers. Compressing these residues in balers makes them easier to handle and reduces storage and transport costs. A lack of knowledge on the interaction between the crop stems and the machine components results in sub-optimal designs and control strategies. Recently manufacturers of agricultural machinery are following the same path that manufacturers in other industries (e.g. automotive and aerospace) have been following for years. Optimization of (agricultural) machines is achieved, more and more, by using models and simulations. As the interactions between individual stems and machine components determine the process behaviour, a modelling framework on this level is required. Discrete Element Modelling (DEM) is a logical choice in this case, as it allows to model the behaviour of each particle (e.g. a crop stem) through its interactions with the other particles and the system elements (Tijskens et al., 2003).

1.1. Discrete element modelling of crop stems

DEM is increasingly used in agricultural applications for simulating particulate processes. The number of studies with bendable crop stems in DEM is, however, very limited. In the few studies where bendable crop stems have been considered, they have been defined by combining different segments

which can move relative to each other. These segments can be spheres (Li et al., 2012; Jünemann et al., 2013), cylinders (Lenaerts et al., 2014; Leblicq et al., 2014) or capsules (Leblicq et al., 2016). The flexible particles in these studies all have linear-elastic bending behaviour.

1.2. Bending of crop stems

To assess whether the existing (linear elastic) models yield realistic results, we investigated the bending behaviour of crop stems in a previous study (Leblicq et al., 2015b). Two consecutive phases could be distinguished during the bending of stems: ovalisation and buckling. During ovalisation, the forces on the wall tend to flatten the cross section of the stem. When a stem is bent, the inner side of the stem is longitudinally compressed, while the outer side is stretched. Both this compression and tension result in a resistance of the stem against the bending moment. As both have a component directed towards the centre of the stem, the stresses cause a flattening of the circular cross-section into an oval shape (Leblicq et al., 2015b). This Ovalisation process is considered to be elastic. When this process continues, the flexural stiffness is reduced until the structure becomes unstable and buckles. A kink is suddenly formed and the cross-section locally completely flattens. This deformed cross section offers virtually no resistance to bending (Calladine, 1989).

1.3. Limitations of the existing bending models

The bending processes (ovalisation and buckling) result in highly non-linear and plastic deformation behaviour. After the initial linear elastic

phase, the force increases at a slower rate and then drops rapidly for a further increase in deformation (Leblicq et al., 2014). Thus, while linear elastic DEM models can describe the reversible bending of straw stems in a realistic way for small deformations, they are inadequate for describing the bending behaviour of crop stems at larger deformations where buckling phenomena become important (Leblicq et al., 2014).

In addition, in all previous studies, the effect of plastic deformation and damaging has never been taken into account. Leblicq et al. (2016), however, showed that crop stalks respond differently to deformation when they already have been deformed plastically. The effect of deformation speed was also never taken into account. Peleg (1983); Faborode & O'Callaghan (1989); Kaliyan & Morey (2009); Nona et al. (2014) showed that the deformation rate influences the bulk compression behaviour. However, no reports were found on the effect of plastic deformation and deformation speed on the bending behaviour of individual crop stems.

1.4. Objectives of this study

The general purpose of this study was to develop and validate a realistic DEM bending model for crop stems. The parameters of the virtual stems should be calibrated using stem measurements to ensure realistic results. The effects of deformation speed, support distance and plastic deformations should also be studied and incorporated in the bending model.

2. Material and methods

Virtual bendable stems were created in the DEMeter++ software, which was previously also used by Lenaerts et al. (2014) and Leblicq et al. (2015a).

In this software, virtual segmented stems consist of connected capsules. A rotational spring is placed between two segments/capsules to create the bending resistance (Fig. 1(a)). When the stem is bent, this rotational spring (k_b) generates a moment (M) that counteracts the bending.

$$M = k_b\theta \tag{1}$$

The bending angle (θ) is chosen such that it is zero when the stem is undeformed and thus the angle increases with increasing deformation. For this, the following definition is used for the bending angle: $\theta = \pi - \phi$. where ϕ is the angle between two segments (Fig. 1(a)). An extra damper (damping constant c) is responsible for stabilizing the simulation by dissipating energy.

$$M = k_b\theta + c\dot{\theta} \tag{2}$$

In this equation $\dot{\theta}$ is the rotational velocity. In contrast to the work of Lenaerts et al. (2014) and Leblicq et al. (2015b) (who used the same software), only one rotational spring is used instead of a large number of axisymmetrically placed extensional springs. Based on the bending moment, forces (F_1 and F_2) are applied to the segments (Fig. 1(b)).

$$\vec{F_1} = \vec{M} \times \vec{L_1} \tag{3}$$

$$\vec{F_2} = -\vec{M} \times \vec{L_2} \tag{4}$$

These forces are added to the other forces acting on the segments to determine the position and velocity of the segments in the next time step.



(a) (b)

Fig. 1. two segments of a virtual stem
(a) bending moment, (b) resulting forces

When the rotational spring (k_b) has a constant value, the virtual stem again behaves linear elastic when bent (as was the case with the axisymmetrically placed extensional springs of Lenaerts et al. (2014) and Leblicq et al. (2016)). To create stems with realistic bending behaviour, the value of k_b should be made variable and depending on the angle and the previous deformation. To determine realistic values, a data-based approach (based on stem measurements) was used. To do this, stem bending measurements were first done.

2.1. Bending measurements

Thirty wheat stems (origination from Issoudun (France), July 2014) were measured. The stems were harvested by hand to reduce early damaging. They were then deformed by three point bending using a single column testing machine (Type LS1 Material Tester, LLoyd materials testing, West Sussex, UK) at a speed of 1 mm/s (Fig. 2). The support distance was set to 50 mm in accordance with Annoussamy et al. (2000); Nazari Galedar et al. (2008); Tavakoli et al. (2009). In order to approximate the shape of a crop stem, the plunger consisted of a solid metal cylinder with a diameter corresponding to that of an average wheat stem (3.5 mm, Leblicq et al. (2015b)).

This geometry was chosen to simulate the bending of a stem due to the interaction with a stem-shaped object. When the plunger moves down, the stem is deformed and the required force is recorded with a 50 N loadcell (Type LS Loadcell 50N, LLoyd Instruments, West Sussex, UK). To determine the effect of plastic deformation and damaging, the procedure suggested by Leblicq et al. (2016) was used. The measurements were not performed in one run, but step-wise. In every cycle, the plunger moves down an additional 0.1 mm relative to the previous cycle and then returns to the initial position. The deformation is thus incrementally increased.

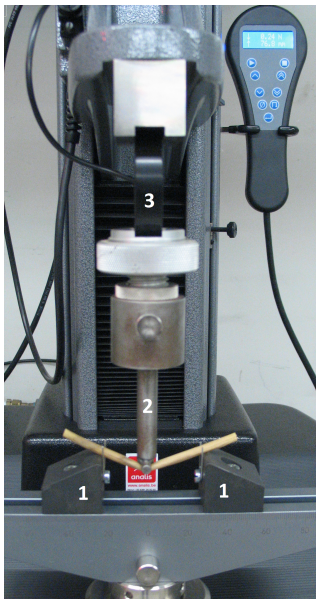

Fig. 2. Measurement set-up for three point bending of a crop stems
1) supports, 2) plunger, 3) load cell

To study the influence of the support distance, next to the thirty stems measured at a support distance of 50 mm (section 2.1), thirty extra stems

(originating from the same field and harvested at the same time) were measured at a support distance of 100 mm following the same procedure.

The influence of the deformation speed could not be studied using the single column testing machine. Preliminary testing showed that the range of deformation speeds (from 10^{-5} m/s to 0.03 m/s), obtained with this machine, was too limited to observe significant differences in the stem bending behaviour. Therefore, a pendulum device (developed by Van Zeebroeck et al. (2003)), which can handle higher deformation speeds, was used to measure bending forces, displacements and displacement rates of a metal plunger during its impact on a crop stem (Fig. 3).

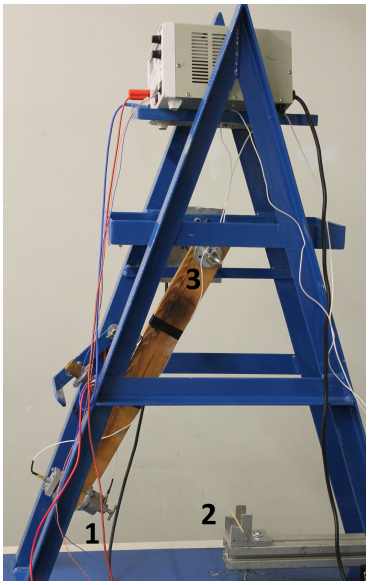

(a)

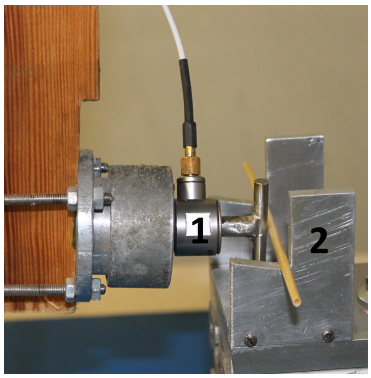

(b)

Fig. 3. Pendulum setup for bending test at high deformation rates.
(1) load cell and plunger, (2) bending support, (3) encoder

The pendulum consists of a 0.495 m long arm with an aluminium tubular impactor at its tip (similar to the plunger of the single column testing machine). The impactor itself is attached to a force sensor (type 1051v3, Dytran Instruments, Chatsworth, USA). At the hinge of the pendulum arm, an incremental optical encoder (type TTLX5, Heidenhain, Traunreut, Germany) is mounted. The stem to be tested is kept in place by two supports 50 mm apart (similar to the three point bending tests at lower deformation rates). By varying the initial angle of the pendulum arm, different impact energies and different deformation rates can be created. Displacement and displacement rate are measured by the encoder, which in fact measures the angular position of the impactor. The tangential displacement of the impactor is calculated from the displacement angle by taking the length of the pendulum arm into account. Three different strain rates were applied (0.54, 1.06 and 1.56 m/s). For each deformation rate thirty stems were measured. Anova testing was used to determine whether the measured stems exhibited significantly different bending behaviour at different speeds. The initial slope, the maximum force and the deformation at maximum force were compared.

2.2. From measured data to DEM models

The stem measurements were then used to obtain realistic values for the springs resisting bending (k_b). The spring should be dependent on the bending angle and the maximum extent to which the stem has been deformed.

$$k_b = f(\theta, \mathrm{MHA}) \tag{5}$$

Where MHA is the maximum historical angle (the largest deformation).

First the data of a bending experiment are divided into two groups: the data where the plunger is moving down and the data where the plunger is retracting. For each measured data point (force (F) as a function of deformation(x)), the bending angle (θ), the maximum historical angle (MHA) and the stiffness of the rotational spring in DEM (k_b) are determined.

The bending angle can be determined from the measured deformation:

$$\theta = \pi - 2\,\mathrm{atan}(\frac{L}{2x})) \tag{6}$$

where L is the support distance.

For each angle also the MHA is determined. During the first cycle, while the plunger is moving down, the MHA is increasing. When the plunger retracts, the MHA stays constant and is equal to the maximum angle of the first cycle. During the second cycle, the MHA will only increase after the plunger has exceeded the maximum angle of the first cycle. The MHA is thus always equal to or larger than the current bending angle.

To determine the values of the rotational spring stiffness (k_b) for each data point, Eq. (1) and the definition of moment of force are combined. In the stem bending experiments, the force was applied in the middle of the supports.The moment of force is then:

$$M = \frac{L}{2}F \tag{7}$$

Combining these equations results in:

$$k_b = \frac{LF_{plunjer}}{2\theta} \tag{8}$$

Each data point now consists of five values: deformation (x), force (F), bending angle (θ), MHA and rotational spring stiffness (k_b). Each pair of values for the bending angle and the MHA corresponds to a rotational spring stiffness. This relation was used to create look up tables (LUT's) from the data.

2.2.1. Look up tables

For each measurement, two equidistant grids (loading and unloading) were formed by the vectors of the MHA and the angle. A grid size of 0.005 rad was used. Linear interpolation between neighbouring points was then used to determine the value of the bending spring for each grid point. For all thirty bending measurements look up tables were built.

Each segment of the virtual stems has a memory, in which the maximum historical angle (MHA) is stored. In every time step of the simulation and for each pair of neighbouring segments, the angle between those segments is determined. For this angle and the stored MHA, the corresponding rotational spring stiffness can be obtained from the look up table. For different angles and for different degrees of historical deformation (MHA), different resistances to bending are thus applied.

$$M = k_b(\theta, \mathrm{MHA})\theta + c\dot{\theta} \tag{9}$$

Depending on whether the deformation increases or decreases, the loading or unloading LUT is used. Leblicq et al. (2016) showed that only taking the previous time step into account to determine whether the deformation is increasing or decreasing is insufficient. High frequency vibrations would

cause a constant switching between LUT's. Therefore, not only the bending angle from the previous time step, but also a weighted change in the bending angle ($d\theta$) is stored per contact. This weighted change of bending angle is calculated as suggested by Janert (2013) and Leblicq et al. (2016):

$$d\theta_t = \frac{d\theta_{t-1} + (\frac{\theta_t - \theta_{t-1}}{\alpha})}{1 + \frac{1}{\alpha}} \tag{10}$$

The parameter α determines the weight of the current time step in the calculation of $d\theta_t$. A higher value of α makes $d\theta_t$ less sensitive to vibrations. A value of 1000 was chosen for α. When $d\theta_t$ is positive, the bending angle is increasing. When $d\theta_t$ is negative, the bending angle is decreasing. The value of $d\theta_t$ determines thus which LUT has to be used.

2.2.2. Other DEM stem parameters

Except for the bending model parameters, all parameters of the virtual stems have been defined similar to those used in Leblicq et al. (2016). For normal compression the databased contact model developed by Leblicq et al. (2016) was used. A normal contact spring (c_c) stabilizes the simulation. The Werner and Haff model (requiring a friction coefficient (μ) and a tangential damper (c_μ)) is used to model the tangential contact forces (friction) (Haff & Werner, 1986). The tensile stiffness of the straw is provided by one spring and damper (k_t, c_t) per segment. The used parameter values are listed in Table 1.

2.3. Stem simulations

To validate the data-based bending models, stem simulations corresponding to the first thirty stem measurements from section 2.1, were conducted.

Table 1. DEM parameters

k_t = spring for tension, c_t = damper for tension, c_c = Damper for compression, μ friction coefficient and c_μ damper for friction

Parameter	Value	Unit
k_t	100	N/m
c_t	0.1	kg/s
c_c	0.1	kg/s
μ	0.3	-
c_μ	10	kg/s

The same support distance (50 mm) was used. Each simulated stem consisted of two segments and was given the LUT's and the diameter from a measured stem. The stems were then bent by a virtual metal plunger. In the simulations, the bending was also performed stepwise (as was the case in the experiments). To demonstrate that the LUT's can generate bending resistances corresponding to angles and MHA's that were not measured, a different step size was used in the simulations than in the measurements.

2.3.1. Influence of the segment length

Eq. (9) and the LUT's (k_b) associated with it, describe the relation between the bending resistance of a pair of segments and the angle between those segments. The equation is not restricted to a specific support distance, number of segments or segment length. Therefore, it is assumed that Eq. (9) can also be used for different configurations (different stem length, different number of segments, different segment length). To validate this assumption, the simulations were repeated with virtual stems consisting of five and ten

segments. Since the support distance (50 mm) was not changed, the segment lengths changed from 25 mm to respectively 10 mm and 5 mm.

2.3.2. Influence of the support distance

The LUT's, created based on the thirty stem measurements at a support distance of 50 mm, were used to simulate the bending of stems at a support distance of 100 mm. The virtual stems consisted of ten segments (segment length of 10 mm in accordance with the median segment length of the previous section). Paired-sample t-tests were then performed to determine whether the thirty extra measured bending profiles (at a support distance of 100 mm) exhibited significantly different bending behaviour than the simulated profiles. For this purpose, the initial slope, the maximum force and the deformation at maximum force were compared.

3. Results and discussion

3.1. Stem measurements

Stem measurements were used to create virtual stems with realistic geometries and realistic bending behaviour. A typical measured stepwise force-deformation profile is displayed in Fig. 4. This measurement shows how the force-deformation behaviour changes due to plastic deformation. It also shows the reaction to the retraction of the plunger and gives information about the hysteresis.

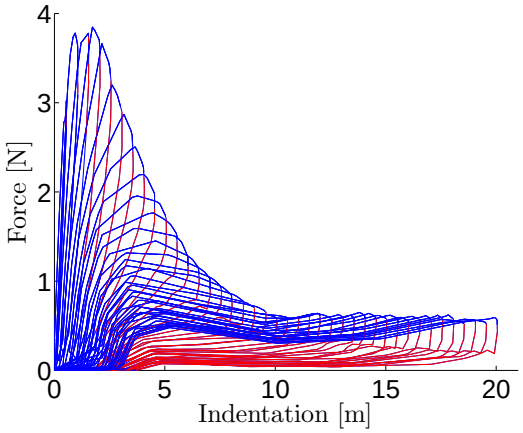

Fig. 4. Stepwise bending (experimental results)

For clarity loading is displayed in blue and unloading is displayed in red

For each measured data point in Fig. 4 (force (F) and deformation(x)) also the bending angle (θ), the maximum historical angle (MHA) and the stiffness of the rotational spring (k_b) are shown in Fig. 5. The calculation of θ, MHA and k_b was done for all thirty measured stems.

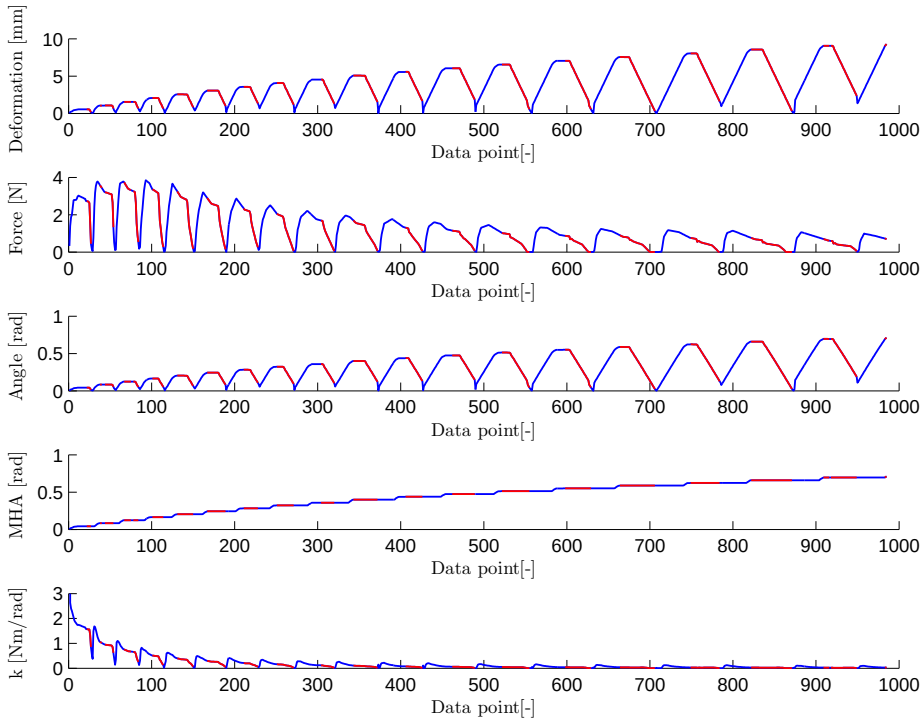

Fig. 5. For each measured data point (consisting of the applied deformation and the resulting force), the corresponding bending angle, the maximum historical angle (MHA) and the stiffness of the rotational spring can be determined.
For clarity loading is displayed in blue and unloading is displayed in red

3.2. Graphical representation of the look up tables

The stepwise deformation data acquired during the bending tests were used to create look up tables. Graphical representations of the look up tables (both loading and unloading) built from the data in Fig. 4 and Fig. 5 are shown in Fig. 6. Each horizontal line represents one cycle in the stepwise deformation. Because the MHA is at least equal to the bending angle, there are no data in the lower right corner. For all thirty first measurements look up tables were built.

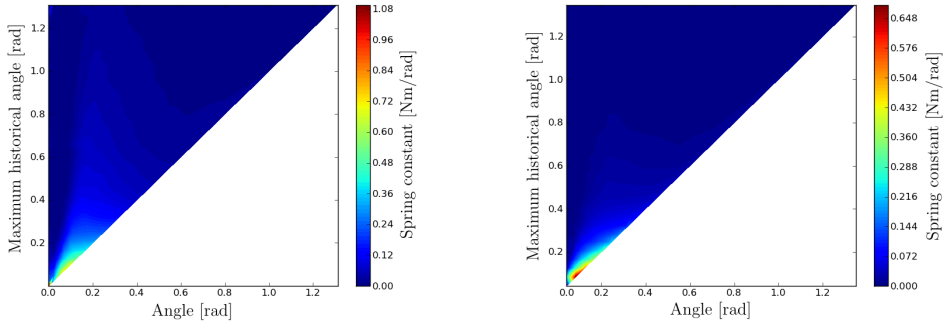

(a) (b)

Fig. 6. Look up tables for the stepwise bending data of Fig. 4 and Fig. 5. (a) loading, (b) unloading

3.3. Stem simulations

3.3.1. Two segments

To validate the bending model, the measurements were repeated in simulation. First, virtual stems consisting of two segments were used. These stems were given the same diameters as those of the measured stems. In Fig. 7, a typical bending measurement (black) and the corresponding simulation (blue) are displayed.

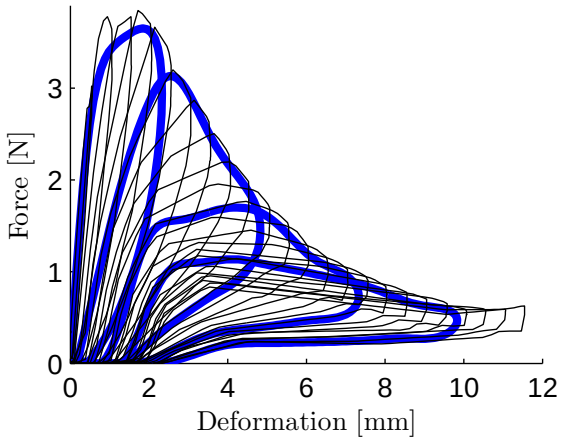

Fig. 7. Stepwise bending profile for a wheat stem (black: measurement, blue: simulation)

A different step size was used in the simulations and in the measurements to demonstrate that the LUT's can generate spring constants and thus forces that were not measured. From Fig. 7 it can be concluded that the simulated bending profiles correspond well with the measured ones. This could have been expected as the bending model is data based. Similar results were obtained for all thirty bending measurements.

3.3.2. Multiple segments

Then, it was studied if, using the same LUT's, stems consisting of more than two segments also produce realistic results. Therefore, the simulations were repeated with virtual stems consisting of five and ten segments. The results (a measurement and three corresponding simulations) are displayed in Fig. 8(a). For visual clearness a global measured profile is also displayed. A global deformation profile consists of the data points with maximum deformation of each cycle. This deformation profile equals the profile which

would have been measured if the test would have been performed in one run (i.e. not stepwise). In accordance with the global deformation profile, the deformation in the simulations is applied in one run.

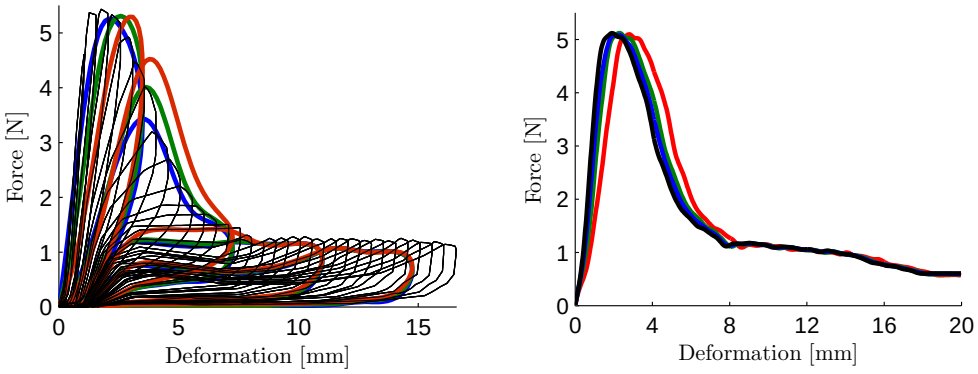

(a) (b)

Fig. 8. Influence of segment length

(a) stepwise deformation, (b) deformation in one run

black: data from three-point bending test of a wheat stem at a support distance of 50 mm, blue: corresponding simulation with virtual stem consisting of two segments, green: corresponding simulation with five segments, red: corresponding simulation with ten segments.

The best agreement with the measured profile is obtained for virtual stems consisting of two segments. The more segments a virtual stems contains, the less accurate the results become (average values for two segments (for the global profiles): RMSE = 0.275 N, $R^2 = 0.969$, five segments: RMSE = 0.325 N, $R^2 = 0.942$ and ten segments: RMSE = 0.424 N, $R^2 = 0.917$). However, it should be noted that, even for larger numbers of segments, the results are still sufficiently accurate for bulk simulations. This was the case for all thirty measured stems (R^2 (for ten segments) was always larger than

0.9). However, it can be noted that the decrease in accuracy only occurs in the first phase of bending (ovalisation). During ovalisation the stem deforms parabolic (Fig. 9(a)). The error arises from the way in which the bending angle is determined during the construction of the LUT (Eq. (6)). For each position of the plunger, and thus for each deformation of the stem, one angle is determined. Here, it is thus implicitly assumed that the stem consists of two segments. However, during ovalisation, there is not one clear bending angle, but a gradient of angles over the length of the stem. During the second phase of bending this no longer is a problem, because after buckling the deformation is concentrated in one location (i.e. in one bending angle (Fig. 9(a))). By implicitly constructing the LUT for two segments, the stem cannot bend parabolically due to a lack of degrees of freedom. When more than two segments are used in the simulations, the stems become less rigid and the curve shifts to the right (Fig. 8). During deformation, all stems, resulting from one measurement, but with different numbers of segments, will follow the same force trajectory. Only the angles will differ slightly. The energy required to deform a stem will therefore almost be equal for different numbers of segments. As a result, the effect of the error on the bulk deformation behaviour will be very small.

Finally, also the geometry of the stems during bending is displayed in Fig. 9. The simulation succeeds in reproducing the effects of ovalisation (parabolic deformation) and buckling. The fact that these effects were not intentionally inserted in the model, but follow automatically from the DEM simulations confirms the potential of this model to realistically simulate the

bending behaviour of crop stems.

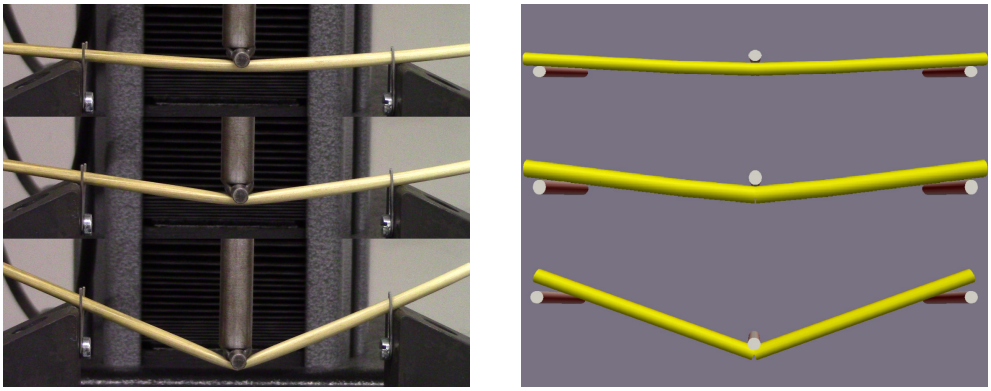

(a) (b)

Fig. 9. Different stages in bending a stem
(a) measurement, (b) simulation

3.4. Influence of stem configuration

To evaluate if Eq. (9) and the associated LUT's can produce realistic results for different support distances, simulations were conducted for a support distance of 100 mm using the LUT's that were created based on the thirty measurements at a support distance of 50 mm. Besides these first thirty stem measurements, an extra thirty stems were measured at a support distance of 100 mm to validate the simulations at a larger support distance. The initial slope, the maximum force and the deformation at maximum force were compared (Fig. 10).

As expected, the measured results (5 cm (M) and 10 cm (M)) differ. When the support distance is larger, a smaller force is required for the same amount of deformation. For the same deflection, a larger support distance results in a smaller bending angle. As a result, a larger deformation is required before

buckling (and F_{max}) occurs. This in turn results in a smaller slope.

T-tests were conducted to determine whether the simulation results (10 cm (S)) were, on average, equal to the new measurements (10 cm (M)). The p-values for the t-tests are: 0.151 (slope), 0.315 (F_{max}) and 0.852 (deformation at F_{max}). The simulations and the validation measurements were thus not significantly different. This means that based on a stem measurement at 50 mm, it can be stimulated what would happen to the same stem if its length would be twice the original length and if it would be supported at a distance twice as long. This was expected since Eq. (9) and the corresponding LUT's only describe the interaction between two segments (i.e. a limited part of the total stem) without taking the length of the entire stem into account .

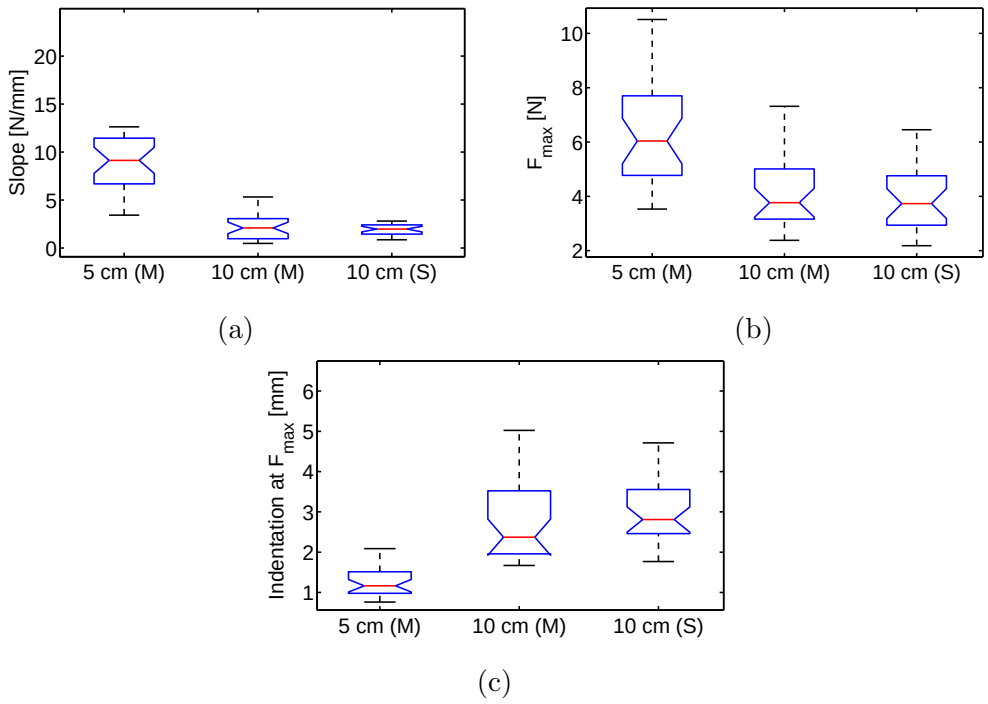

Fig. 10. Comparison of measured and simulated bending profiles

(a) comparison of the initial slopes, (b) comparison of the maximum forces, (c) comparison of the deformations at maximum force

5 cm (M): 30 wheat stems measured at a support distance of 5 cm, 10 cm (M): 30 wheat stems measured at a support distance of 10 cm, 10 cm (S): 30 simulated bending tests at support distance of 10 cm (the stem properties came from the measurements at a support distance of 5 cm).

3.5. Effect of deformation speed

To study the influence of deformation speed on the bending behaviour of crop stems, pendulum experiments were conducted. Three different deformation rates were applied (0.54, 1.06 and 1.56 m/s). For each deformation rate, thirty stems were measured. Anova analysis was then used to determine whether the force-deformation profiles were significantly different. The initial

slope, the maximum force and the deformation at maximum force were again compared (Fig. 11). The p-values from the anova tests are: 0.421 (slope), 0.2345 (F_{max}) and 0.186 (deformation at F_{max}). So, no significant effect of the deformation speed could be observed. However, several researchers have observed an effect of speed on the deformation behaviour at the bulk level (Peleg, 1983; Faborode & O'Callaghan, 1989; Kaliyan & Morey, 2009; Nona et al., 2014). It is hypothesized here that this effect is caused by the interaction of different stems and not by the deformation of individual stems. Different consecutive phases occur during bulk compression of crops (Leblicq et al., 2015b). In the first phase the stems rearrange and the air voids among stems are filled. It is hypothesised that friction plays the most important role during this phase. In the following phases the stems are bent and compressed. The way in which stems rearrange during compression (and thus the way in which the material deforms as a bulk) can still be speed-dependent although the deformation of individual stems is not. The friction between stems, the geometries and the orientations of the stems would then be of major importance.

4. Conclusions

In this study, a data-based approach was used to create a realistic bending model for virtual crop stems in DEM. For this purpose, look up tables were created from stem measurements. These measurements were performed stepwise to assess the influence of plastic deformation. The method was successfully validated for stems with different numbers of segments, for different stem lengths, for different support distances and for stems with different

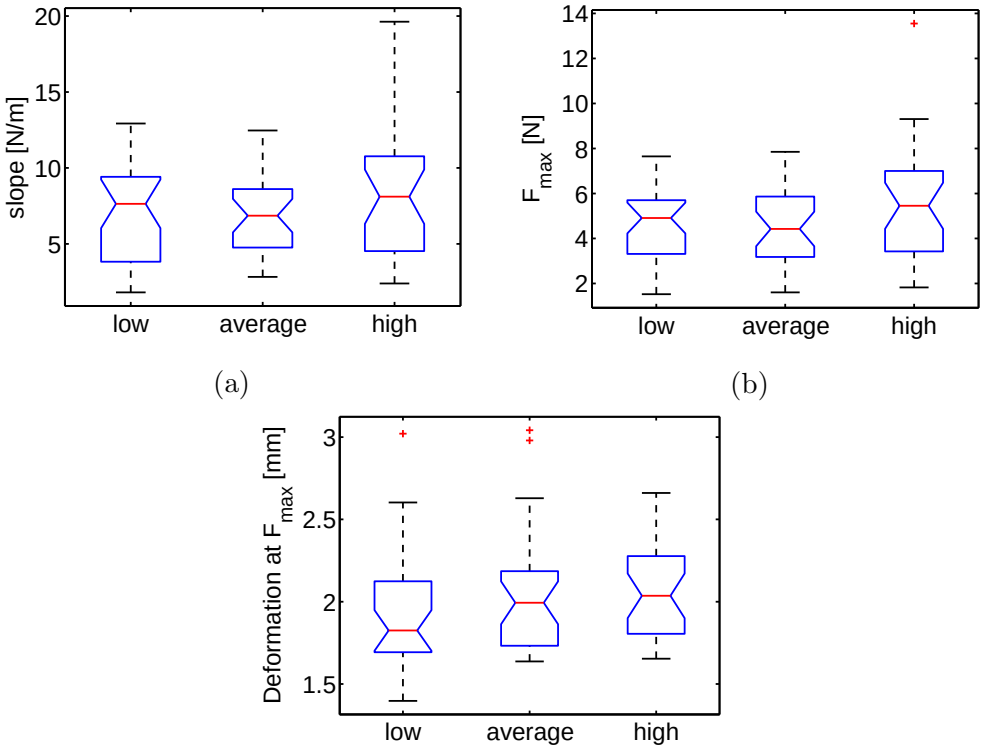

Fig. 11. Comparison of bending profiles at different deformation rates
(a) comparison of the initial slopes, (b) comparison of the maximum forces, (c) comparison of the deformations at maximum force
Slow: 0.54 m/s, average: 1.06 m/s, fast: 1.56 m/s

degrees of plastic deformation. The effect of strain rate was studied using a pendulum device, but no significant differences were found for different deformation speeds.

5. Acknowledgements

The authors wish to thank IWT / KU Leuven IOF for support in the development of Demeter++. Also thanks to Bert De Marrez for his help in making the bending model.

6. References

Annoussamy, M., Richard, G., Recous, S., & Gurif, J. (2000). Change in mechanical properties of wheat straw due to decompositon and moisture. *Applied Engineering in Agriculture*, *16*, 657–664.

Calladine, C. R. (1989). *Theory of shell structures*. Cambridge University Press.

Faborode, M., & O'Callaghan, J. (1989). A rheological model for the compaction of fibrous agricultural materials. *Journal of Agricultural Engineering Research*, *42*, 165–178.

Haff, P., & Werner, B. (1986). Computer simulation of the mechanical sorting of grains. *Powder Technology*, *48*, 239–245.

Janert, P. K. (2013). *Feedback Control for Computer Systems*. O'Reilly Media Inc. Sebastopol, CA. USA.

392 Jünemann, D., Kemper, S., & Frerichs, L. (2013). Simulation of stalks in agri-
393 cultural processes applications of the discrete element method. *Landtech-*
394 *nik*, *68*, 164–167.

395 Kaliyan, N., & Morey, R. V. (2009). Constitutive model for densification of
396 corn stover and switchgrass. *Biosystems engineering*, *104*, 47–63.

397 Leblicq, T., Smeets, B., Ramon, H., & Saeys, W. (2016). A discrete element
398 approach for modelling the compression of crop stems. *Computers and*
399 *Electronics in Agriculture*, *123*, 80–88.

400 Leblicq, T., Vanmaercke, S., Ramon, H., & Saeys, W. (2014). A discrete
401 element model for realistic bendable straw. In *Proc. Int. Conf. Agricul-*
402 *tural Engineering, AgEng2014, 6.-10.07.2014, Zurich. Eur. Soc. Ag. Eng.*
403 *(EurAgEng)*.

404 Leblicq, T., Vanmaercke, S., Ramon, H., & Saeys, W. (2015a). Discrete
405 element modelling of bendable tubes. *International Journal of Mechanical*
406 *Sciences*, *94–95*, 75–83.

407 Leblicq, T., Vanmaercke, S., Ramon, H., & Saeys, W. (2015b). Mechanical
408 analysis of the bending behaviour of plant stems. *Biosystems Engineering*,
409 *129*, 87–99.

410 Lenaerts, B., Aertsen, T., Tijskens, E., De Ketelaere, B., Ramon, H.,
411 De Baerdemaeker, J., & Saeys, W. (2014). Simulation of grain–straw
412 separation by discrete element modeling with bendable straw particles.
413 *Computers and Electronics in Agriculture*, *101*, 24–33.

Li, H., Li, Y., Gao, F., Zhao, Z., & Xu, L. (2012). Cfd–dem simulation of material motion in air-and-screen cleaning device. *Computers and electronics in agriculture*, *88*, 111–119.

Nazari Galedar, M., Jafari, A., Mohtasebi, S., Tabatabaeefar, A., Sharifi, A., O'Dogherty, M., Rafiee, S., & Richard, G. (2008). Effects of moisture content and level in the crop on the engineering properties of alfalfa stems. *Biosystems Engineering*, *101*, 199–208.

Nona, K., Lenaerts, B., Kayacan, E., & Saeys, W. (2014). Bulk compression characteristics of straw and hay. *Biosystems Engineering*, *118*, 194–202.

Peleg, K. (1983). A rheological model of nonlinear viscoplastic solids. *Journal of Rheology*, *27*, 411–431.

Tavakoli, H., Mohtasebi, S., & Jafari, A. (2009). Effects of moisture content, internode position and loading rate on the bending characteristics of barley straw. *Journal of Agricultural Engineering Research*, *55*, 45–51.

Tijskens, E., Ramon, H., & De Baerdemaeker, J. (2003). Discrete element modelling for process simulation in agriculture. *Journal of sound and vibration*, *266*, 493–514.

Van Zeebroeck, M., Tijskens, E., Van Liedekerke, P., Deli, V., De Baerdemaeker, J., & Ramon, H. (2003). Determination of the dynamical behaviour of biological materials during impact using a pendulum device. *Journal of sound and vibration*, *266*, 465–480.